IEEE-CSC, ESAS, and CSSJ SUPERCONDUCTIVITY NEWS FORUM (global edition), October 2023.
Invited presentation given at EUCAS 2023, Sept. 5, 2023, Bologna, Italy

EUCAS2023
Bologna, Italy
3rd-7th September

Fe-based superconducting thin films and their potential for high field applications

Kazumasa Iida (Nihon University)

2023.09.05

Supported by
科研費 KAKENHI (16H04646, 20H02681)
JST CREST 戦略的創造研究推進事業 Core Research for Evolutionary Science and Technology PMJCR18J4)

Contributors

NdFeAsO thin films: K. Kondo, M. Chen, T. Hatano, H. Ikuta

Dept. Materials Physics, Nagoya University

(Ba,K)122 thin films: D. Qin, M. Naito, A. Yamamoto

Dept. of Applied Physics, Tokyo University of Agriculture & Technology

Microstructure: Z. Guo, H. Gao, H. Saito, S. Hata

Dept. of Advanced Materials Science & The Ultramicroscopy Research Center, Kyushu University

High-field transport properties: C. Tarantini, J. Hänisch

ASC NHMFL & Florida State University

Inst. for Technical Physics, Karlsruhe Institute of Technology

Iron based superconductors (IBSs)

FeAs or FeSe or FeTe tetrahedron

✓ Common structure

✓ Important role for superconductivity

FeSe or FeTe tetrahedron

11 | 111 | 1111 | 11111 | 122

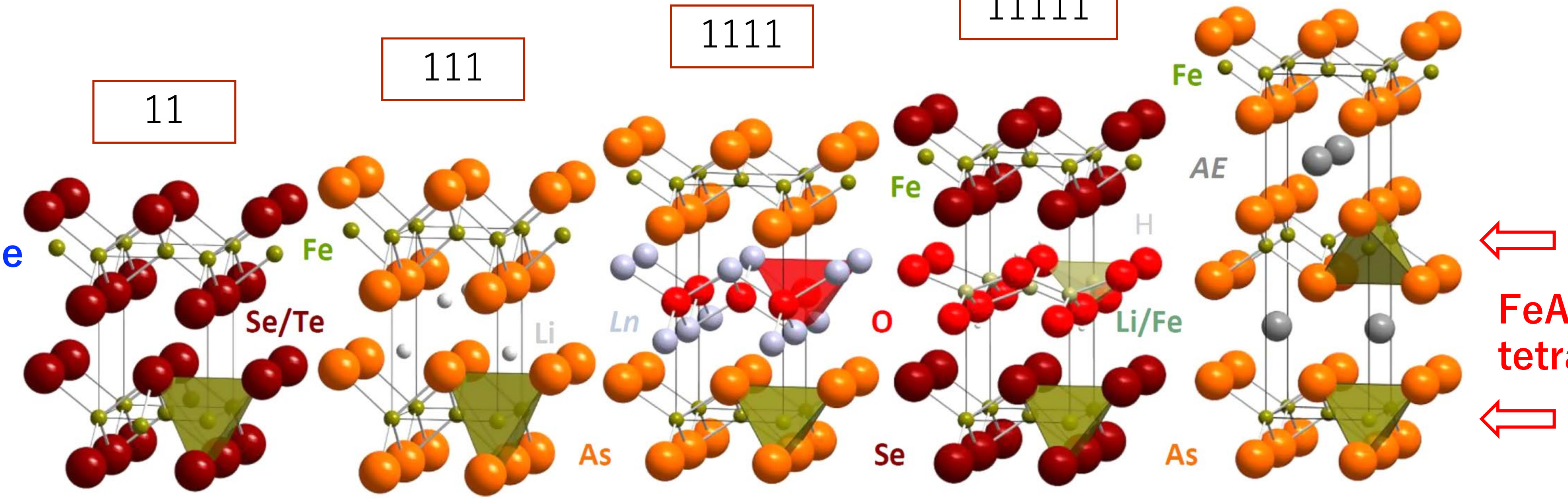

FeAs tetrahedron

11	111	1111	11111	122
Fe(Se,Te)	LiFeAs	*Ln*FeAs(O,F)	(Li,Fe)OHFeSe	$AEFe_2As_2$
T_c^{max}~15 K	T_c^{max}~18 K	T_c^{max}~56 K	T_c^{max}~43 K	T_c^{max}~38 K

J. Hänisch, K. Iida, C. Tarantini, R. Hühne, *Sust* **32**, 093001 (2020).

Iron based superconductors (IBSs)

FeAs or FeSe or FeTe tetrahedron

✓ Common structure

✓ Important role for superconductivity

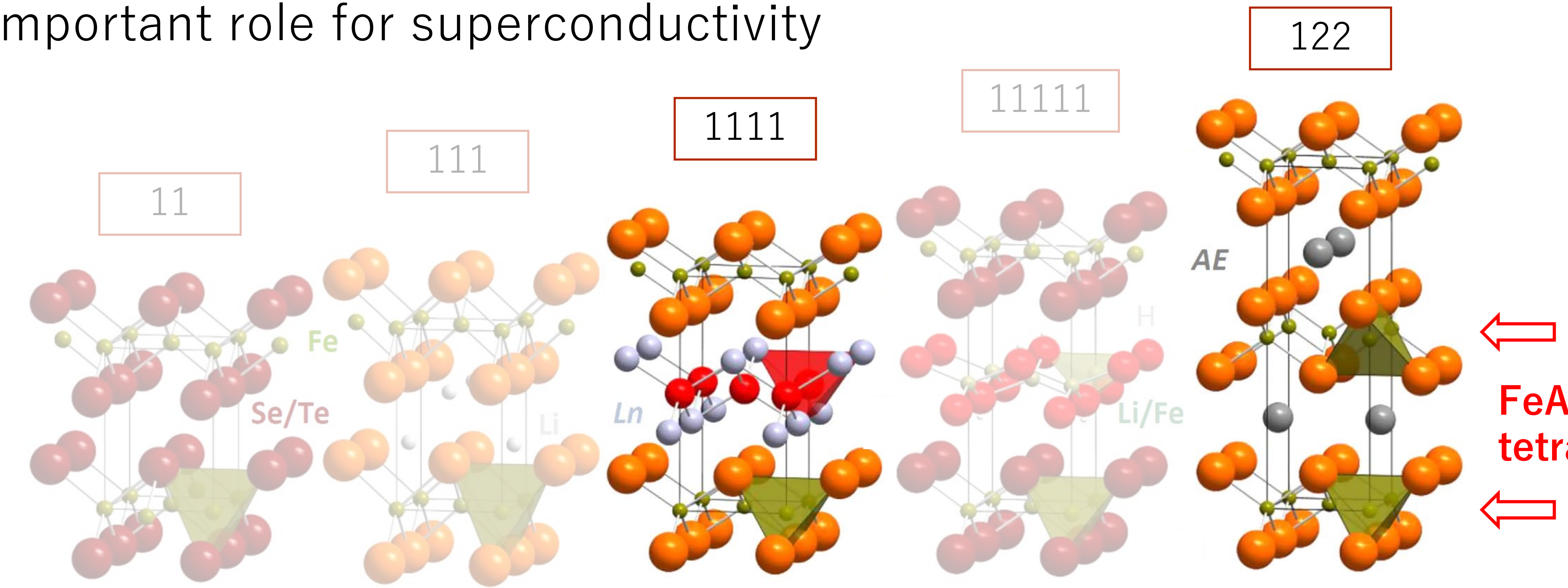

FeAs tetrahedron

11	111	1111	11111	122
Fe(Se,Te)	LiFeAs	*Ln*FeAs(O,F)	(Li,Fe)OHFeSe	*AE*Fe_2As_2
T_c^{max}~15 K	T_c^{max}~18 K	T_c^{max}~56 K	T_c^{max}~43 K	T_c^{max}~38 K

J. Hänisch, K. Iida, C. Tarantini, R. Hühne, *Sust* **32**, 093001 (2020).

IEEE-CSC, ESAS, and CSSJ SUPERCONDUCTIVITY NEWS FORUM (global edition), October 2023.
Invited presentation given at EUCAS 2023, Sept. 5, 2023, Bologna, Italy

Iron based superconductors (IBSs)

FeAs or FeSe or FeTe tetrahedron

- ✓ Common structure
- ✓ Important role for superconductivity

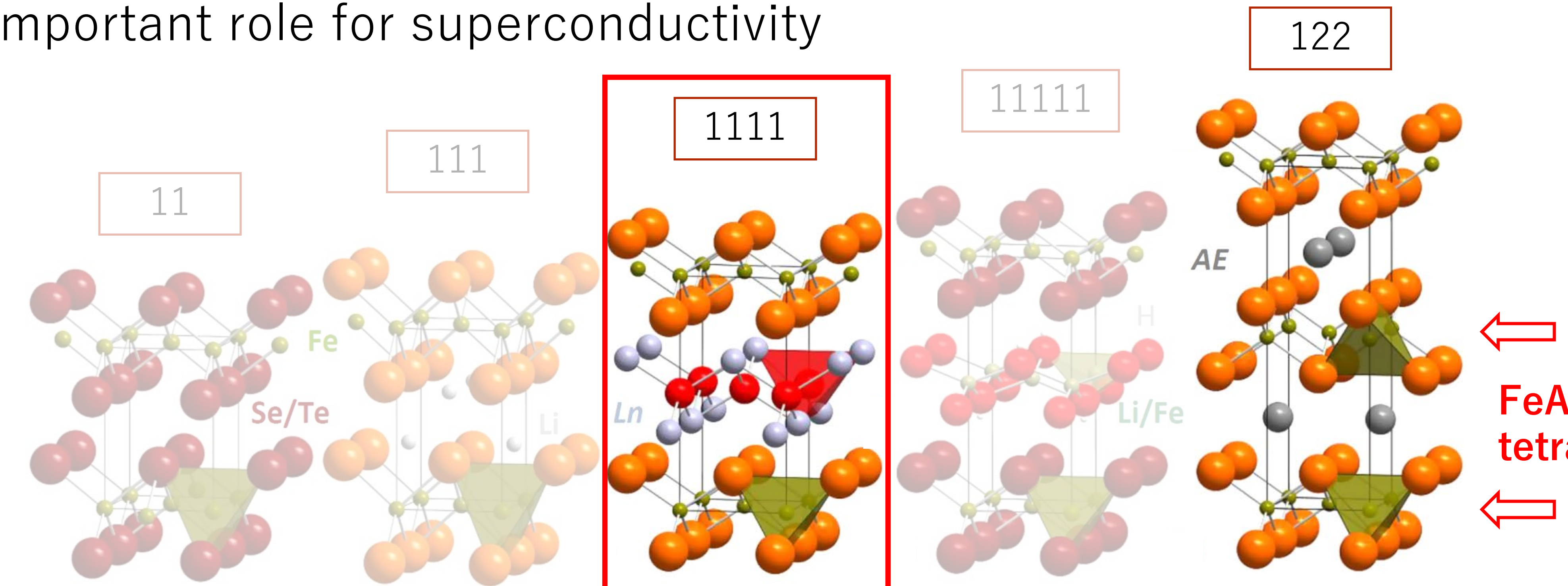

11	111	1111	11111	122
Fe(Se,Te)	LiFeAs	*Ln*FeAs(O,F)	(Li,Fe)OHFeSe	*AE*Fe_2As_2
T_c^{max}~15 K	T_c^{max}~18 K	T_c^{max}~56 K	T_c^{max}~43 K	T_c^{max}~38 K

FeAs tetrahedron

J. Hänisch, K. Iida, C. Tarantini, R. Hühne, *Sust* **32**, 093001 (2020).

Progress of J_c-H for NdFeAs(O,F) (Nd-1111)

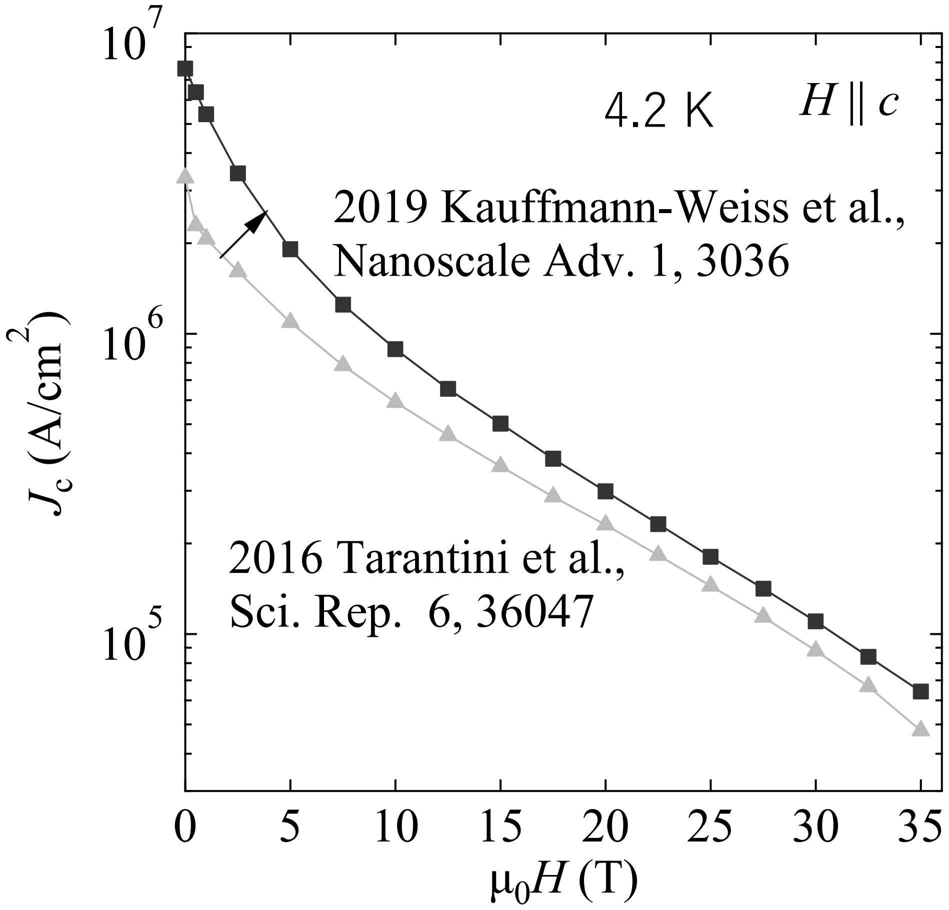

✓ J_c~8 MA/cm^2 for NdFeAs(O,F)

Measured J_c is around 10~20% of J_d

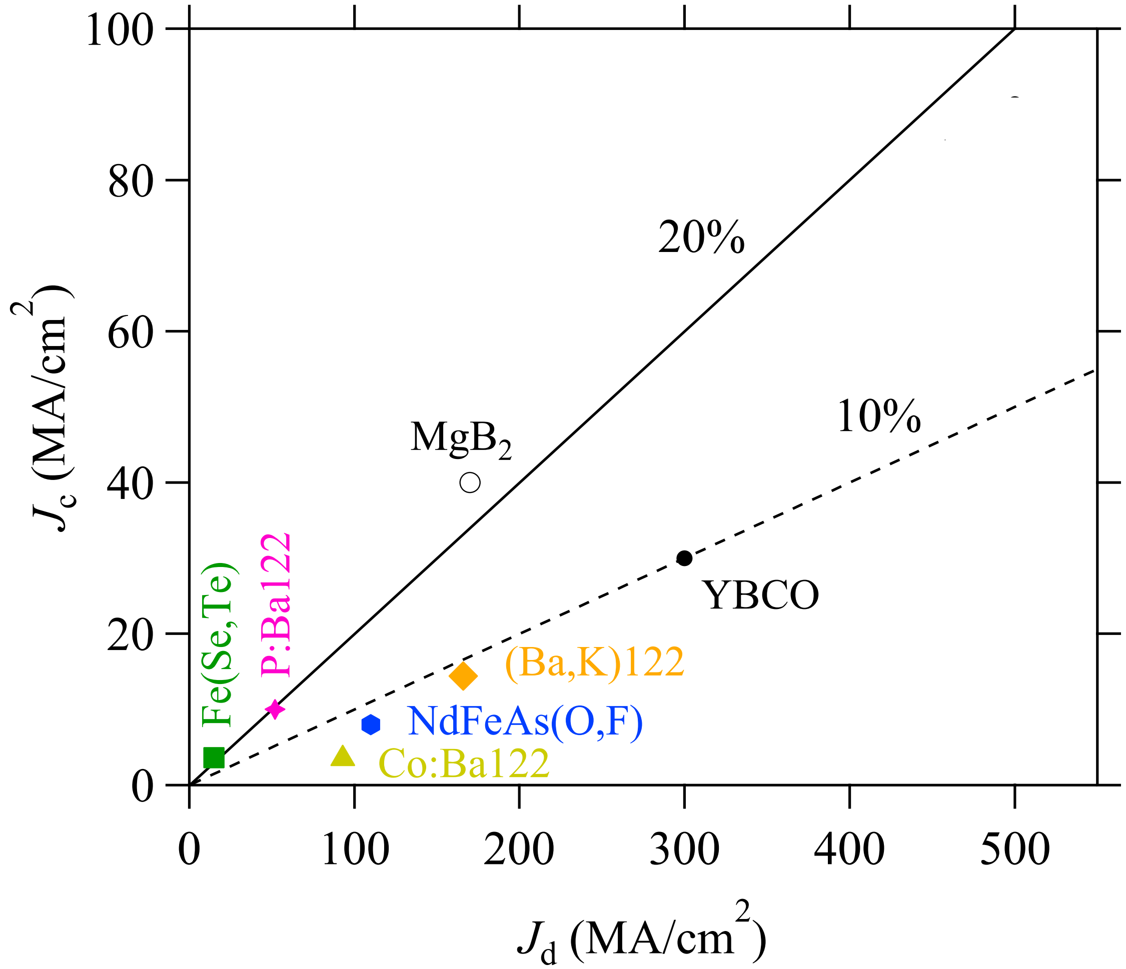

- ✓ J_c~8 MA/cm^2 for NdFeAs(O,F)
- ✓ Higher the J_d, higher the J_c
- ✓ Depairing current density J_d (theoretical upper limit)

$$J_\mathrm{d}(T) = \frac{\phi_0}{3\sqrt{3}\pi\mu_0\lambda^2(T)\xi(T)}$$

Over-doping increases the condensation energy

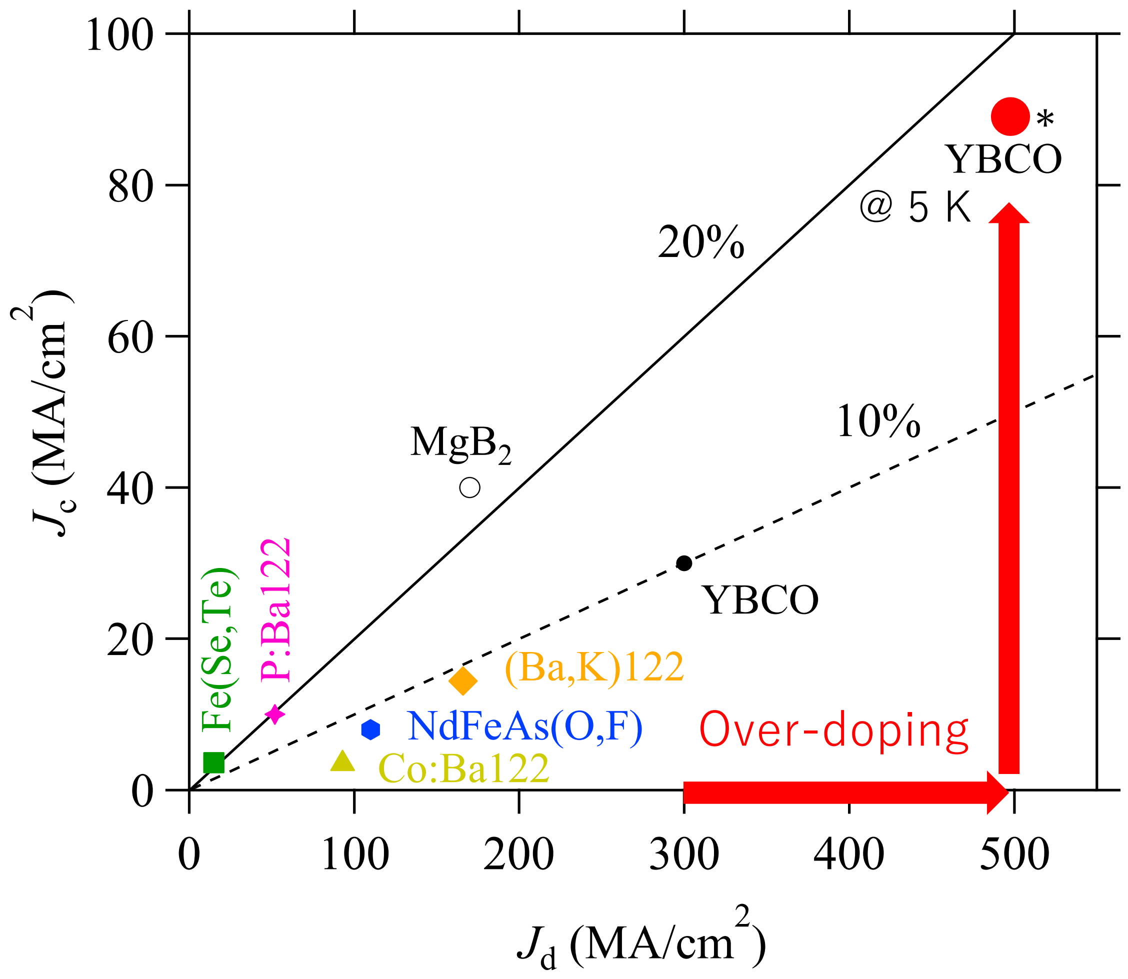

- ✓ J_c~8 MA/cm^2 for NdFeAs(O,F)
- ✓ Higher the J_d, higher the J_c
- ✓ Depairing current density J_d (theoretical upper limit)

$$J_d(T) = \frac{\phi_0}{3\sqrt{3}\pi\mu_0\lambda^2(T)\xi(T)}$$

- ✓ Over-doping increase J_d, and hence J_c

* A. Stangl *et al.*, *Sci. Rep.* ***11***, 8176 (2021).

Combining over-doping and microstructural modification

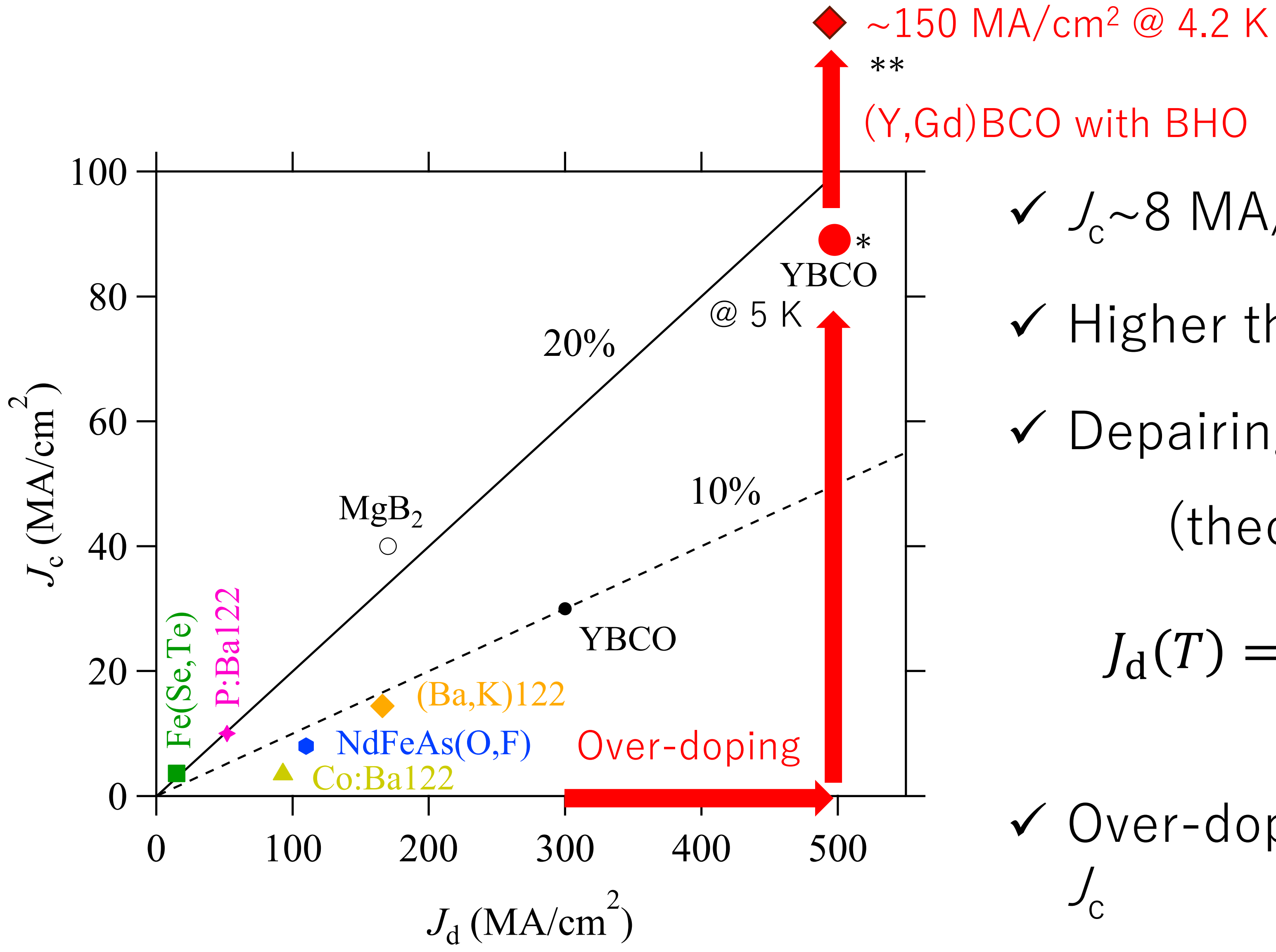

- ✓ J_c~8 MA/cm² for NdFeAs(O,F)
- ✓ Higher the J_d, higher the J_c
- ✓ Depairing current density J_d

  (theoretical upper limit)

$$J_d(T) = \frac{\phi_0}{3\sqrt{3}\pi\mu_0\lambda^2(T)\xi(T)}$$

- ✓ Over-doping increase J_d, and hence J_c

* A. Stangl *et al*., *Sci. Rep.* ***11***, 8176 (2021).

** M. Miura et al., *NPG Asia Mater.* **14**, 85 (2022).

Solubility limit depends on F and H

*Ln*FeAsO (*Ln*: lanthanoide)

$O^{2-} \rightarrow \mathbf{F}^{-}$ or $\mathbf{H}^{-} + e^{-}$ (electron doping)

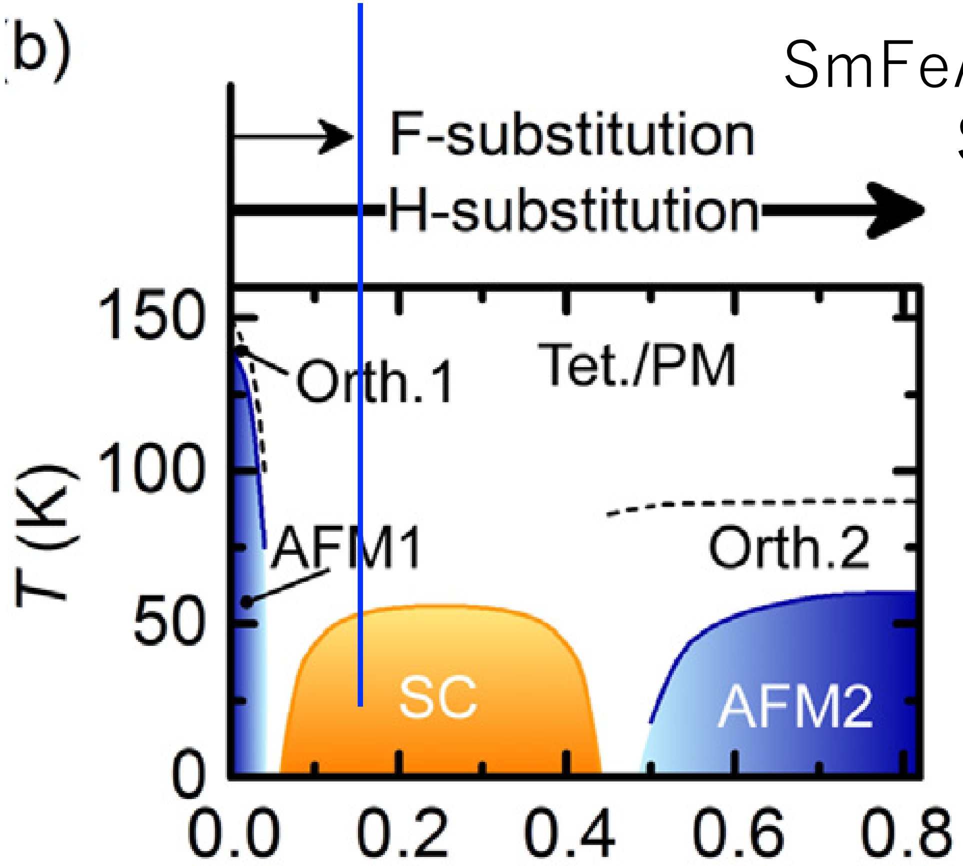

$SmFeAsO_{1-x}\mathbf{F}_x$

$SmFeAsO_{1-x}\mathbf{H}_x$

S. Iimura *et al.*, *J. Asia Ceramic Societies* **5**, 357 (2017).

- Substitution level is limited **up to ~0.2** (For $SmFeAsO_{1-x}F_x$)
- For H, the substitution level is increased **up to ~0.8**
- Heavily electron doped film can be obtained
- T_c keeps constant around 50 K up to x=0.4

*Ln*FeAsO: penetration depth and coherence length

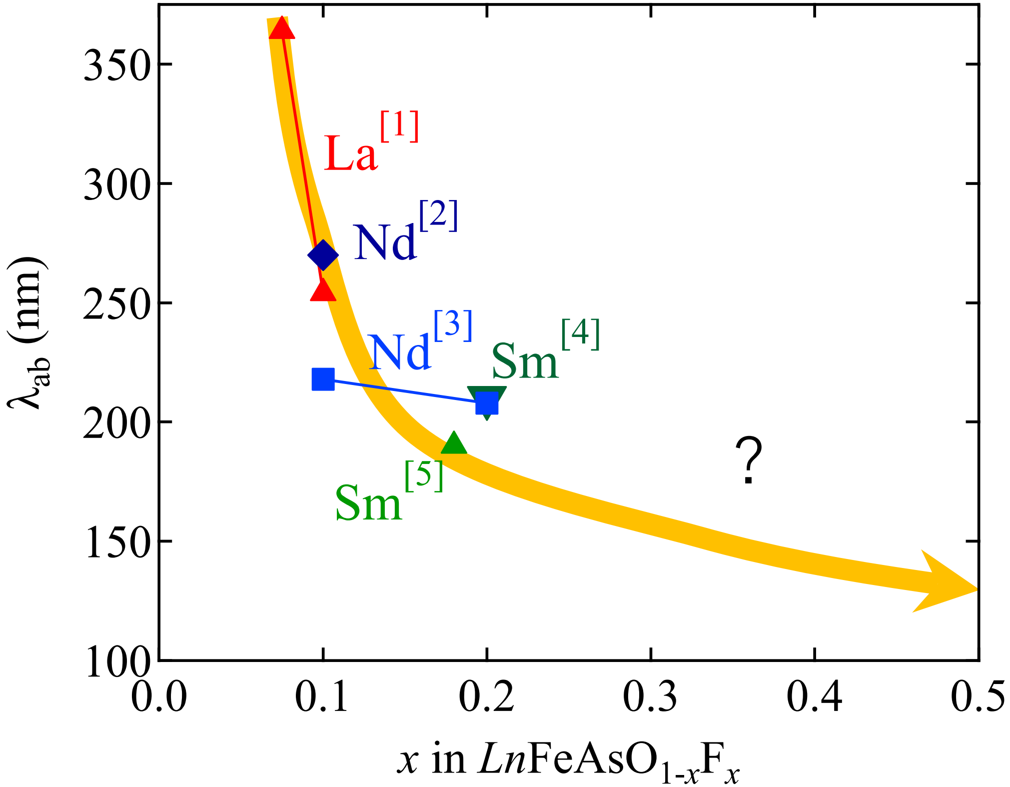

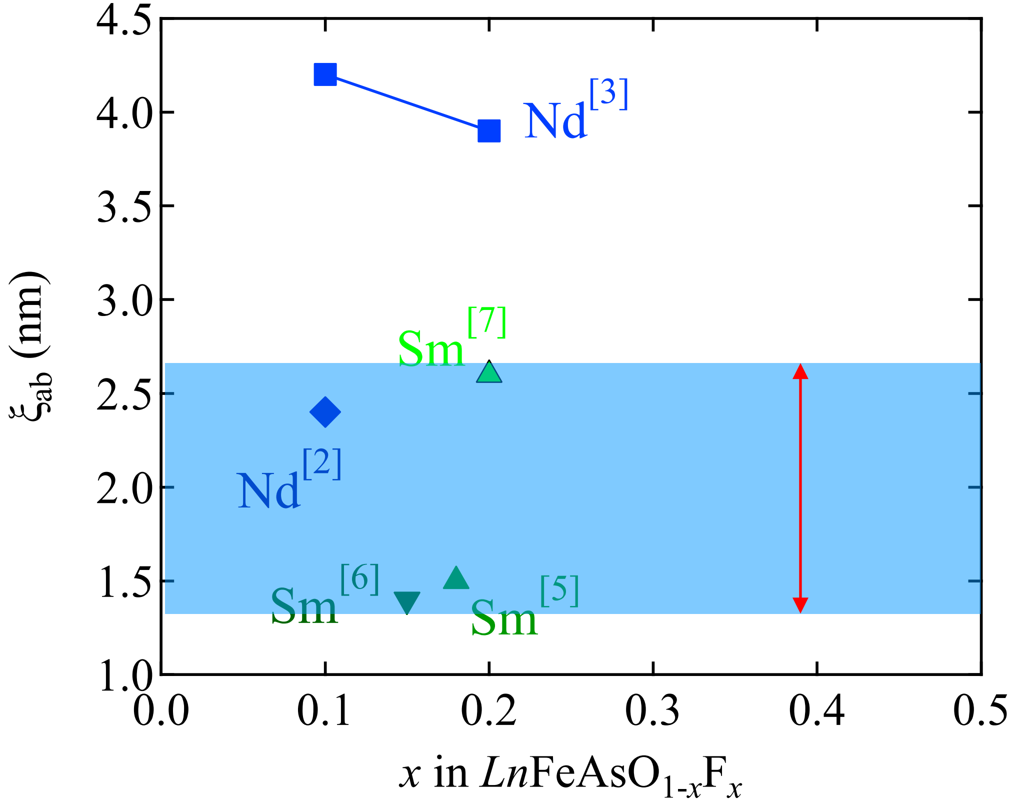

- ➢ λ of *Ln*FeAsO may be decreased with electron doping
- ➢ No clear relation between ξ and electron doping

[1] H. Luetkens *et al.*, *Phys. Rev. Lett.* **101**, 097009 (2008).
[2] J. Kacmarcik *et al.*, *Phys. Rev. B* **80**, 014515 (2009).
[3] A. Adamski *et al.*, *Phys. Rev. B* **96**, 100503 (2017).
[4] S. Weyeneth *et al.*, J. Supercond. Nov. Magn. **22**, 325 (2009).
[5] A. J. Drew *et al.*, *Phys. Rev. Lett.* **101**, 097010 (2008).
[6] U. Welp *et al.*, *Phys. Rev. B* **83**, 100513 (2011).
[7] H-S. Lee *et al.*, *Phys. Rev. B* **80**, 144512 (2009).

Growth of F- and H-doped NdFeAsO thin films

$NdFeAsO_{1-x}F_x$

parent NdFeAsO

$NdFeAsO_{1-x}H_x$

Nd(O,F) overlayer

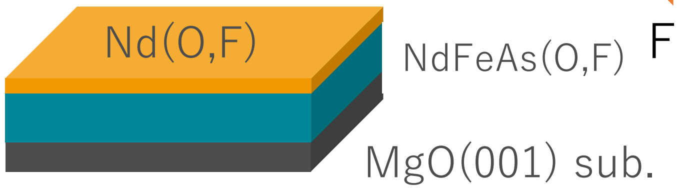

F^- O^{2-}

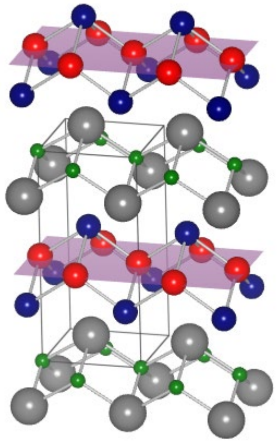

H^- O^{2-}

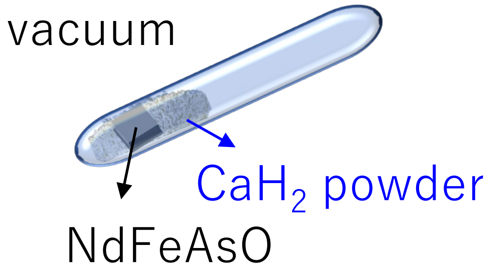

T. Kawaguchi *et al.*, *Appl. Phys. Express* **4**, 083102 (2011).

heat treatment

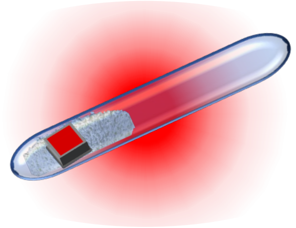

400~500°C
up to 72 h

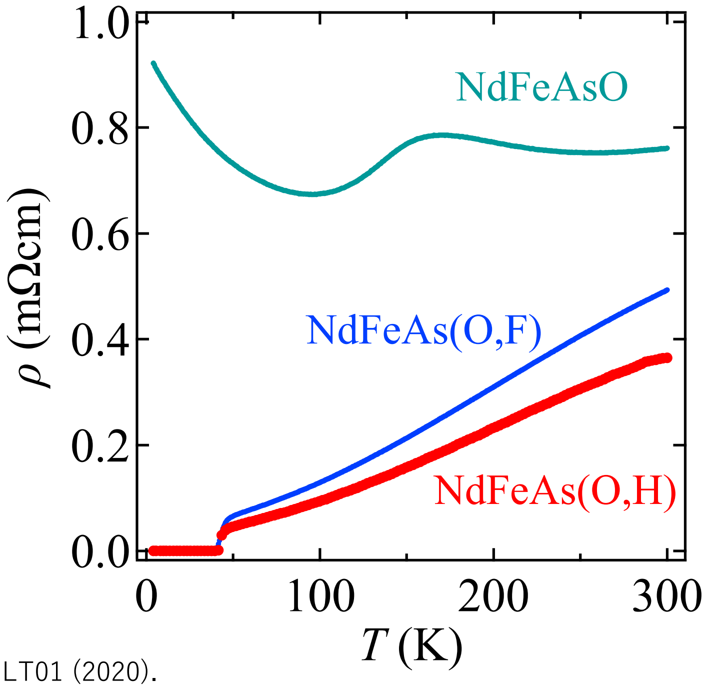

K. Kondo, K. Iida *et al.*, *SuST* ***33***, 09LT01 (2020).

Phase pure & *c*-axis oriented

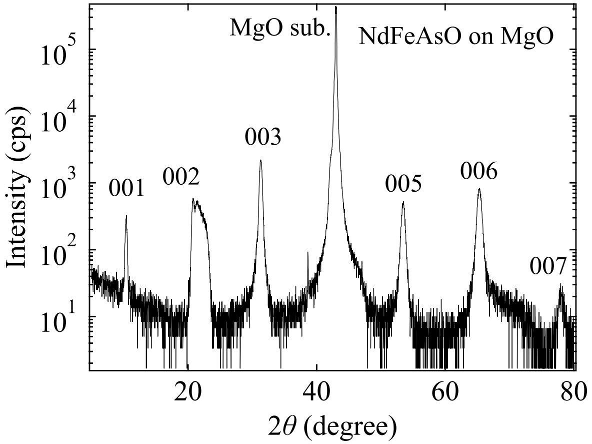

d~24 nm

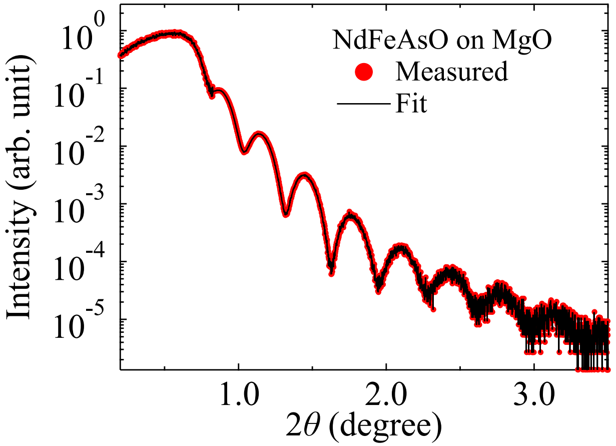

Comparison between H- and F-doping: T_c and carrier density

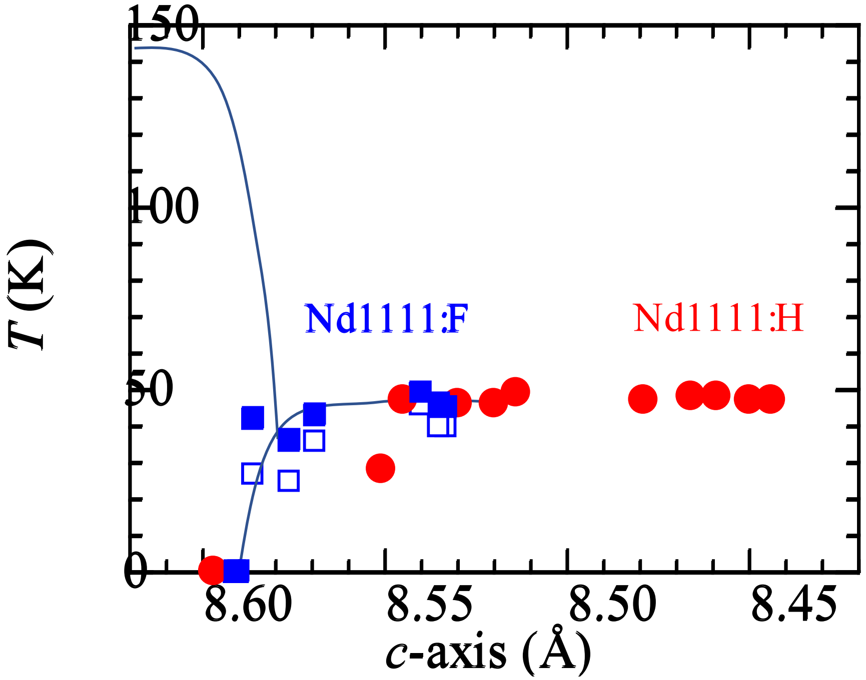

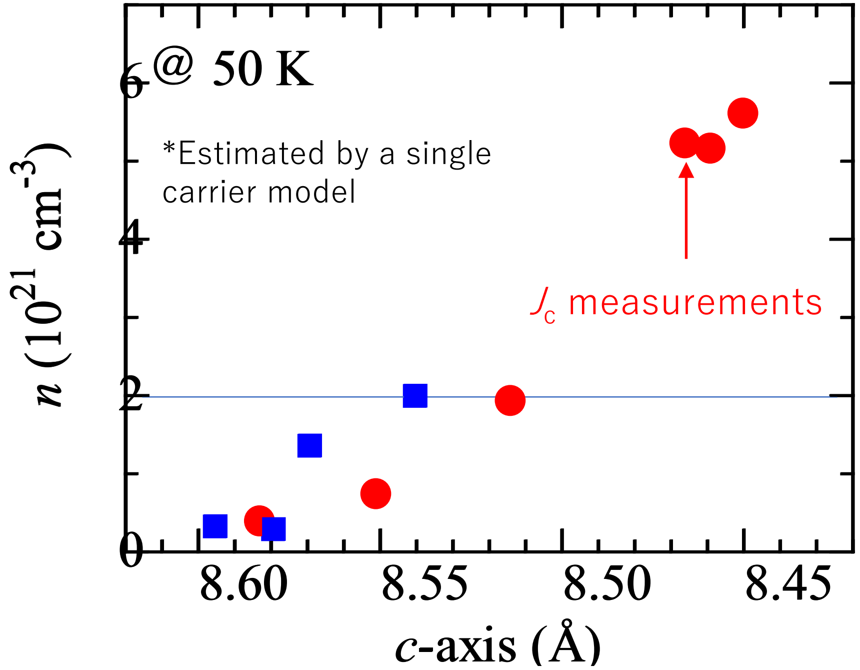

- ➢ A constant T_c of ~ 50 K up to c~8.54 Å, corresponding to carrier density n~2×10^{21} /cm^3
- ➢ c varied in a wide range, 8.44 Å and 8.55 Å with T_c~50 K [NdFeAs(O,H)]
- ➢ The maximum n was around 6×10^{21} /cm^3 [almost 3 times higher than NdFeAs(O,F)]

K. Kondo, K. Iida *et al.*, *Sust* ***33***, 09LT01 (2020).

J_c-H for NdFeAs(O,H) is higher than that for NdFeAs(O,F)

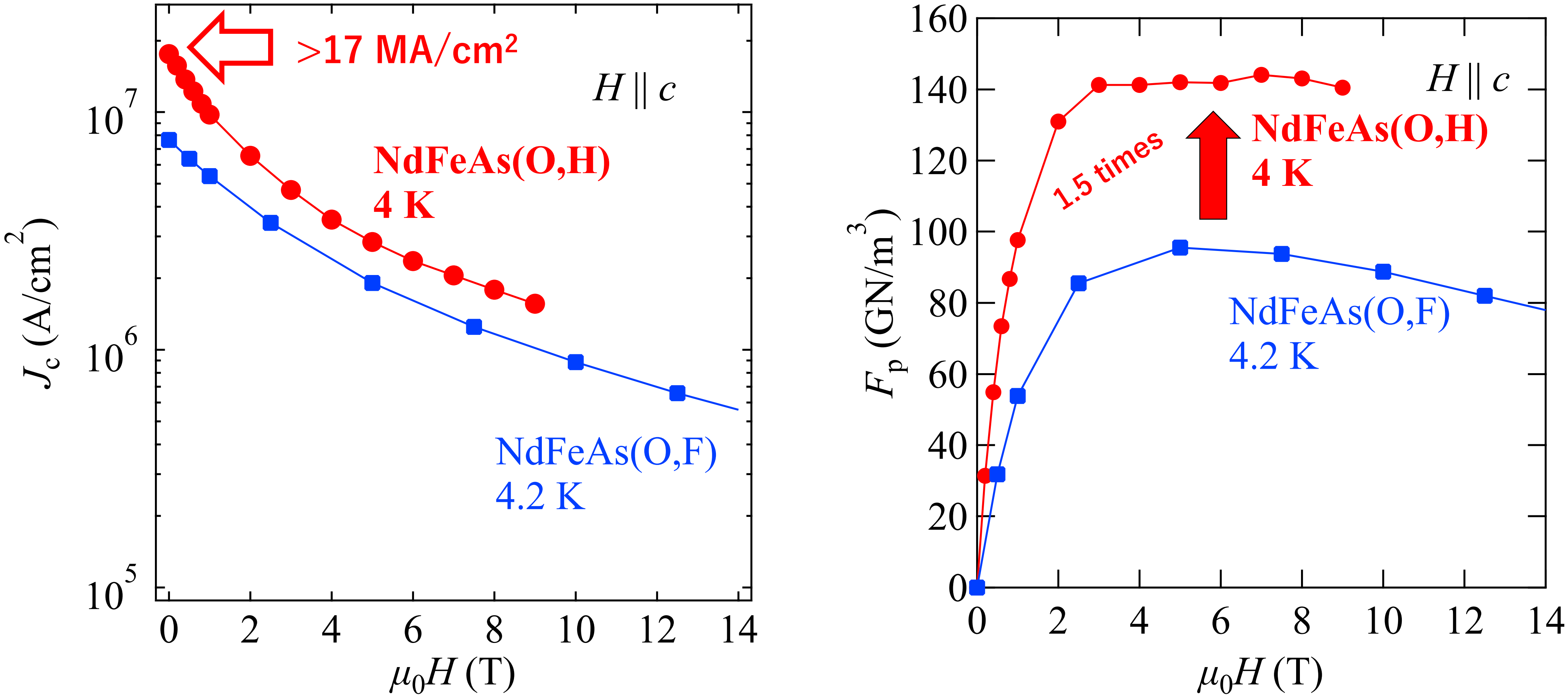

- ➢ J_c(4 K, 0 T)>**17 MA/cm^2**, which is twcie larger than NdFeAs(O,F)

  c.f.) 20 MA/cm^2 for the irradiated SmFeAs(O,F) single crystal [1]

- ➢ F_p of NdFeAs(O,H) is 1.5 times higher than that of NdFeAs(O,F)

F. Fang *et al.*, *Nat. Commun.* *4*, 2655 (2013).

NdFeAs(O,H) shows higher H_{irr} than NdFeAs(O,F)

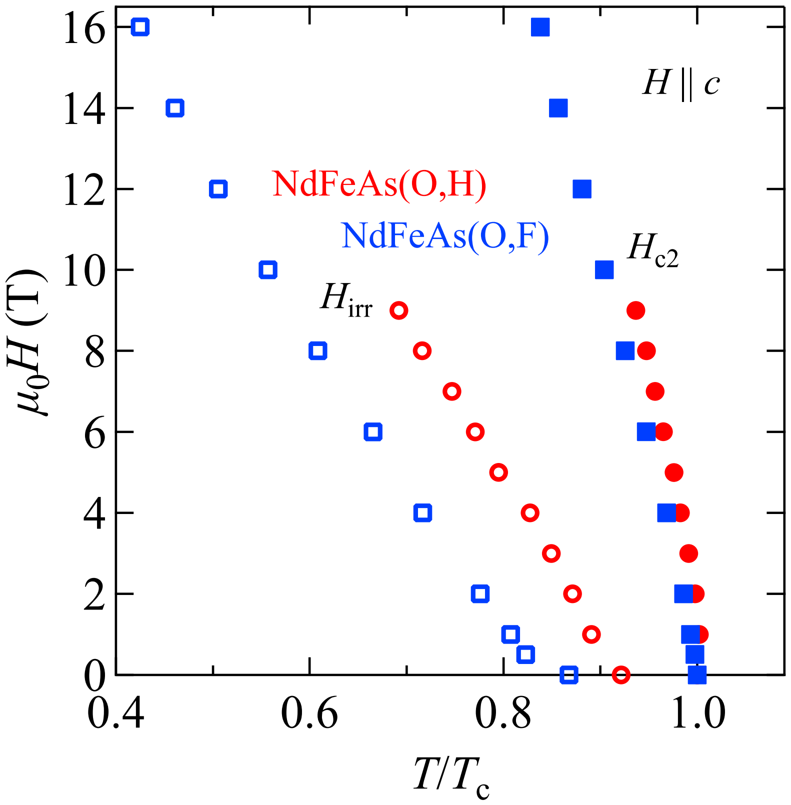

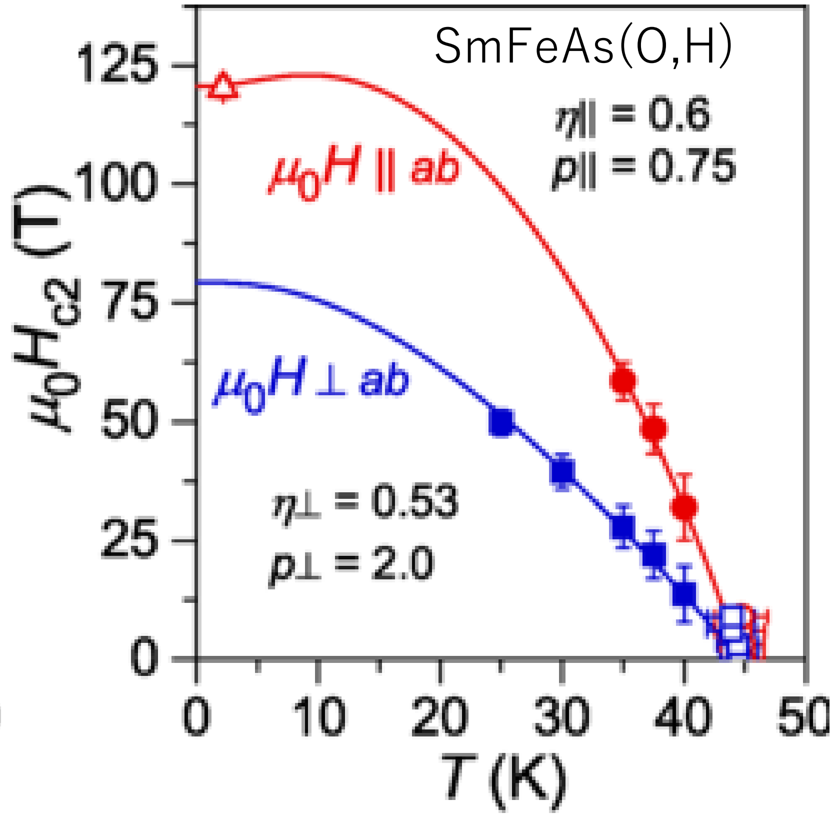

Hanzawa *et al.*, *PRM* **6**, L111
(2022).

- Upper critical field H_{c2} of NdFeAs(O,H) is almost comparable to that of NdFeAs(O,F)
- Irreversibility field H_{irr} of NdFeAs(O,H) is higher than that of NdFeAs(O,F)

-> Due to the decrease in the anisotropy $H_{irr} \propto \frac{H_{c2}}{\gamma^2}$ for $H \parallel c$

Band calculation

Fully substituted H and F of 1111

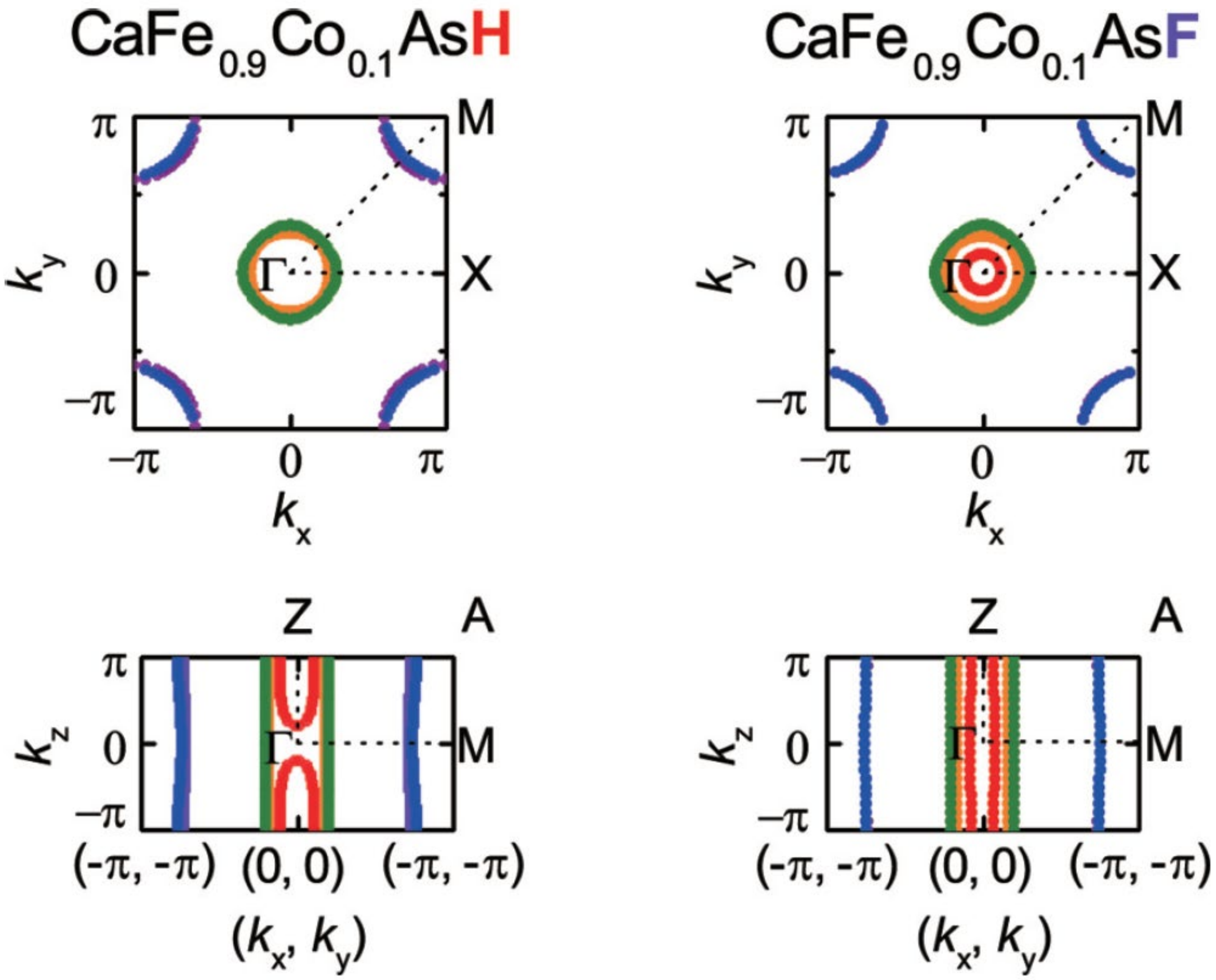

Y. Muraba *et al., PRB* **89**, 094501 (2014).

Evolution of band structure with H

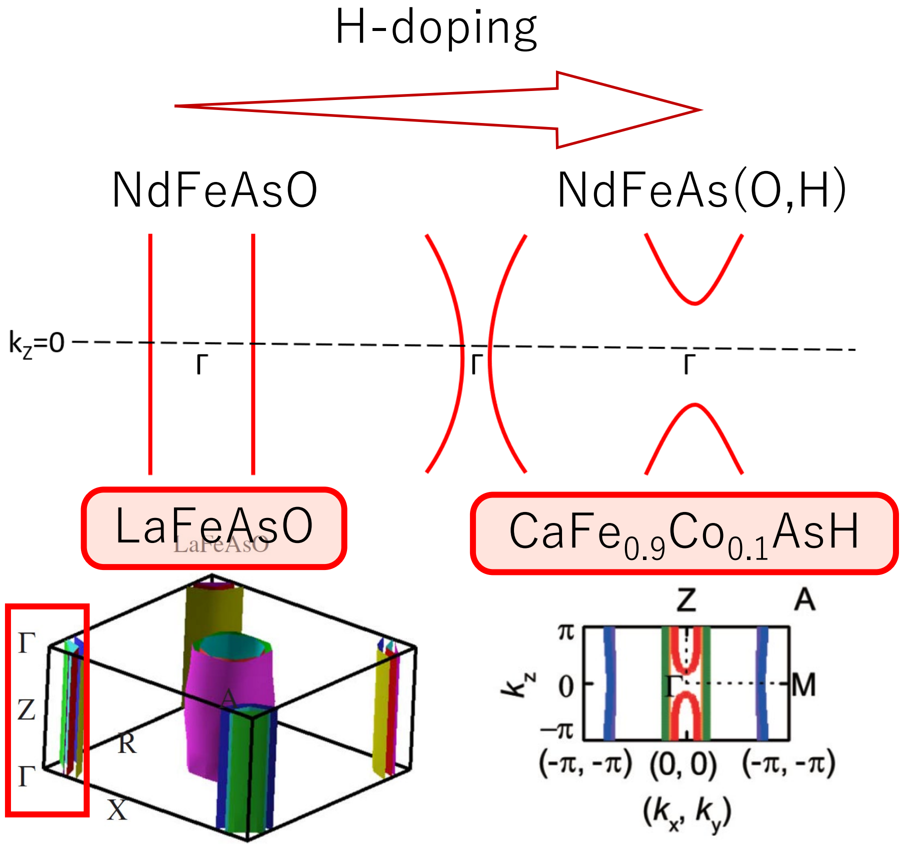

V. Vildosola *et al., PRB* **78**, 064518 (2008).

$(Ba,K)Fe_2As_2$

K-doped *AE*Fe_2As_2 : Only epitaxial thin film has not been realised

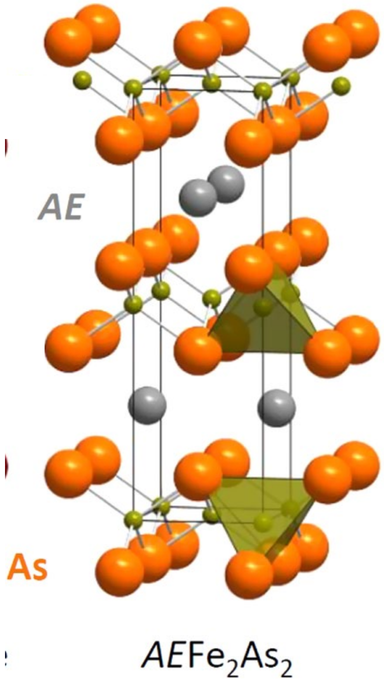

- ✓ T_c^{max}~38 K
- ✓ J_d~170 MA/cm²
- ✓ $\gamma \sim 1-2$

Single crystals

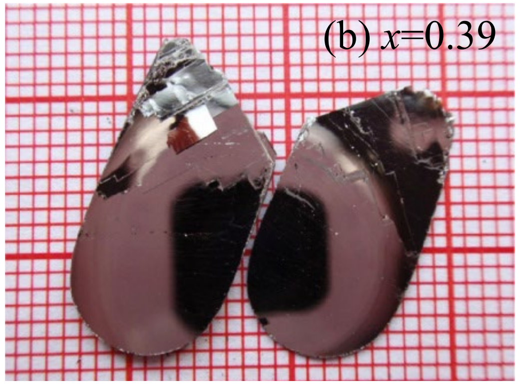

Y. Liu *et al.*, *PRB* ***89***, 13504 (2014).

Wires

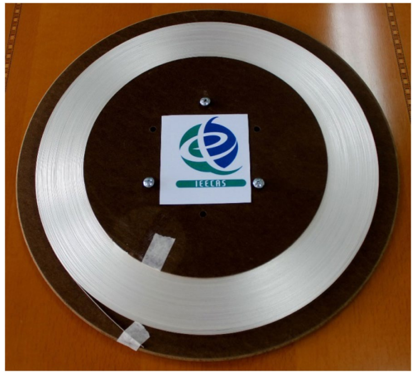

H. Hosono *et al.*, *Mater. Today* ***21***, 278 (2018).

Polycrystalline bulk

J. Weiss *et al.*, *SuST* ***28***, 112001 (2015).


Missing piece

Epitaxial thin film

- ✓ High T_c ~ 38 K, high J_d~170 MA/cm² & low electromagnetic anisotropy
- ✓ The most promising material for applications (e.g. PIT wires and bulk magnets)
- ✓ All material forms except for epitaxial thin films have been available

K-doped Ba122 epitaxial thin film on CaF_2 sub.

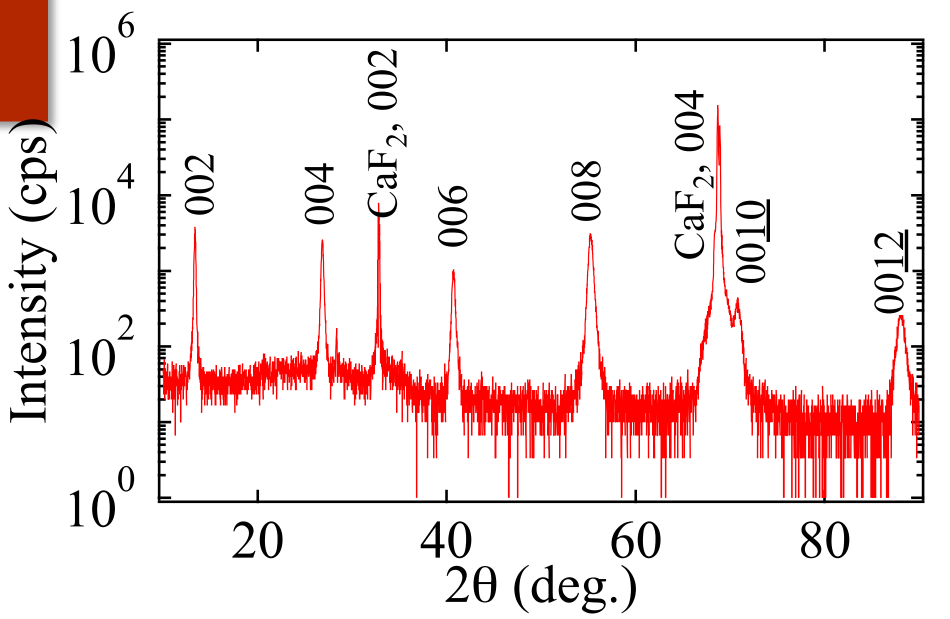

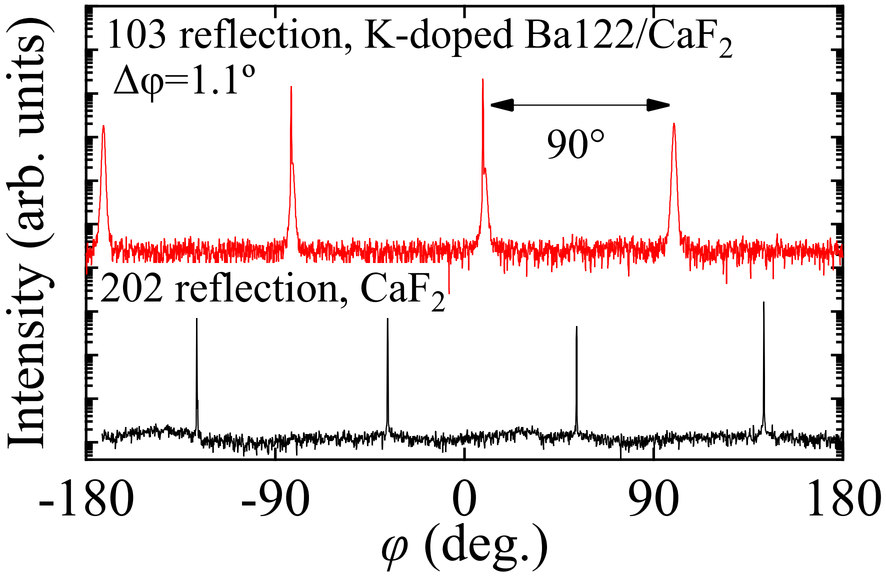

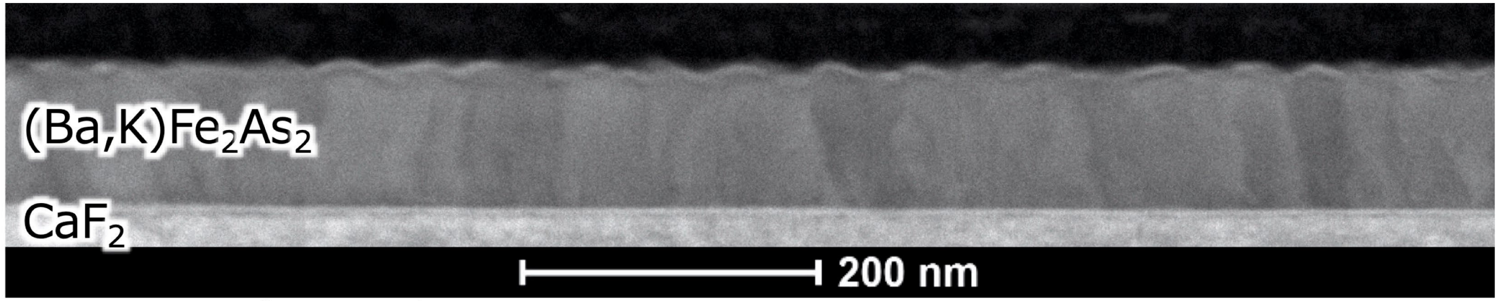

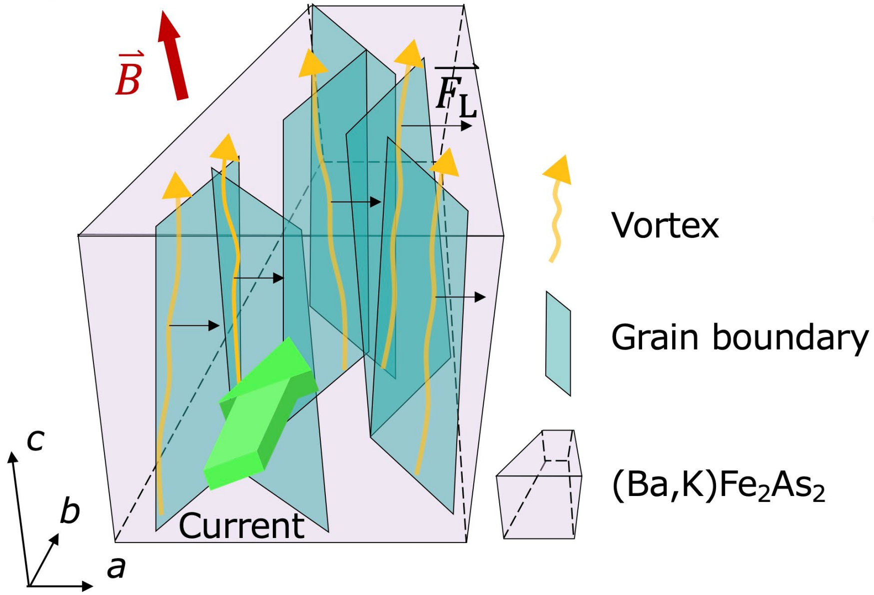

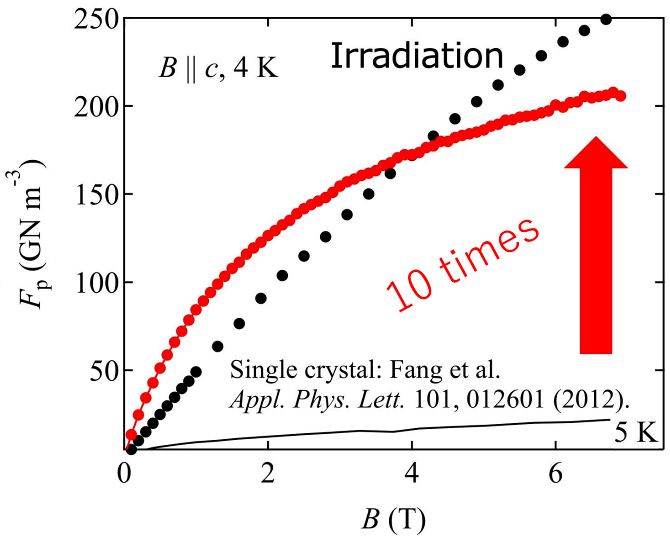

Single crystal: Fang et al. *Appl. Phys. Lett.* 101, 012601 (2012).

Fluoride sub. & **low growth temperature** (~400° C) **are the key to epitaxial growth**

D. Qin *et al.*, *Phys. Rev. Mater.* **5**, 014801 (2021).

K. Iida *et al.*, *NPG Asia Materials* **13**, 68 (2021).

Toward bi-crystal K-doped Ba122 experiments

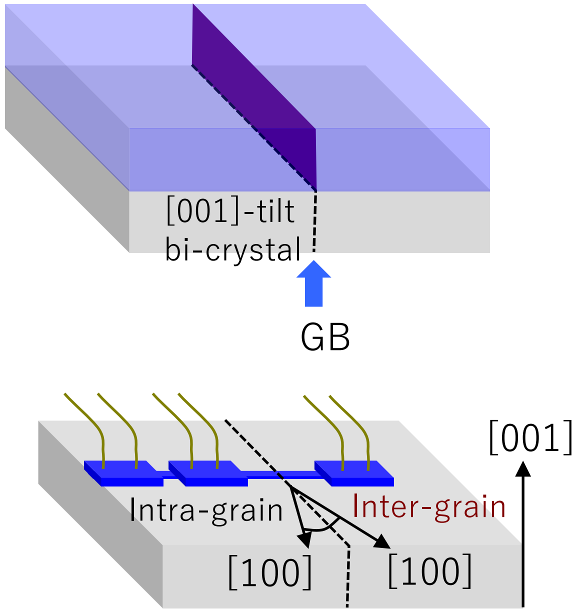

Substrates	Bi-crystal
CaF_2 (001)	Not available
MgO (001)	Available
$SrTiO_3$ (001)	Available

Substrates	Bi-crystal
LSAT[1] (001)	Available
Al_2O_3 (0001)	Available

[1] $La_{0.3}Sr_{0.7}Al_{0.65}Ta_{0.35}O_3$

Toward bi-crystal K-doped Ba122 experiments

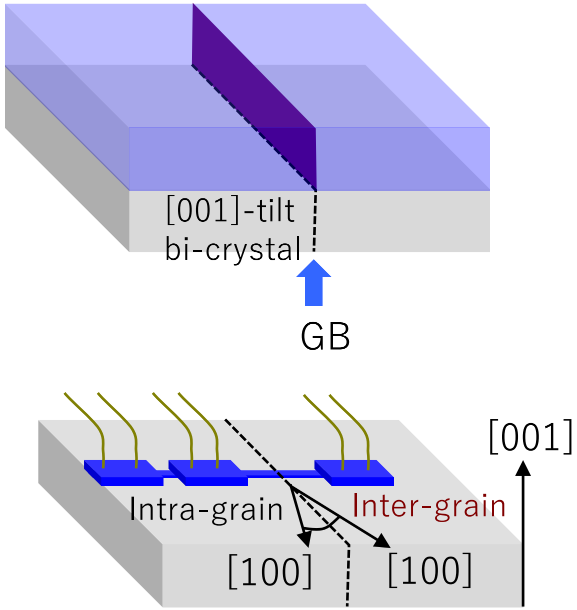

Substrates	Bi-crystal
CaF_2 (001)	Not available
MgO (001)	Available
$SrTiO_3$ (001)	Available

Substrates	Bi-crystal
LSAT (001)	Available
Al_2O_3 (0001)	Available

[1] $La_{0.3}Sr_{0.7}Al_{0.65}Ta_{0.35}O_3$

- ☹ Oxygen is released during deposition ($SrTiO_3$)
- ☹ Reaction layer is present at the interface (LSAT)
- ☺ Ba122 grows epitaxially on MgO

K-doped Ba122 grown on MgO(001)

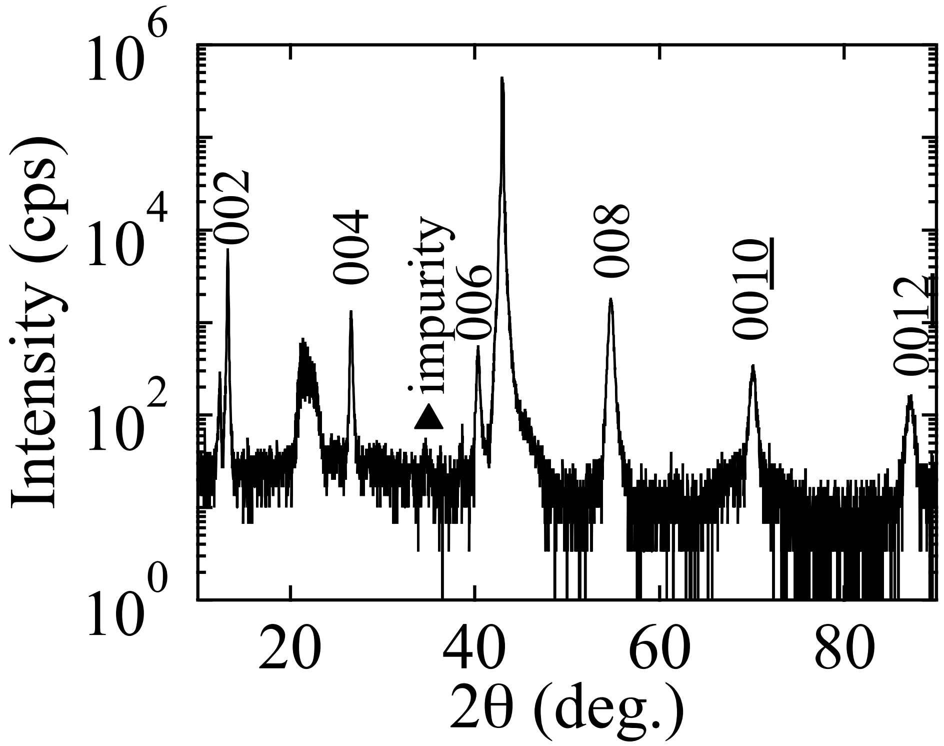

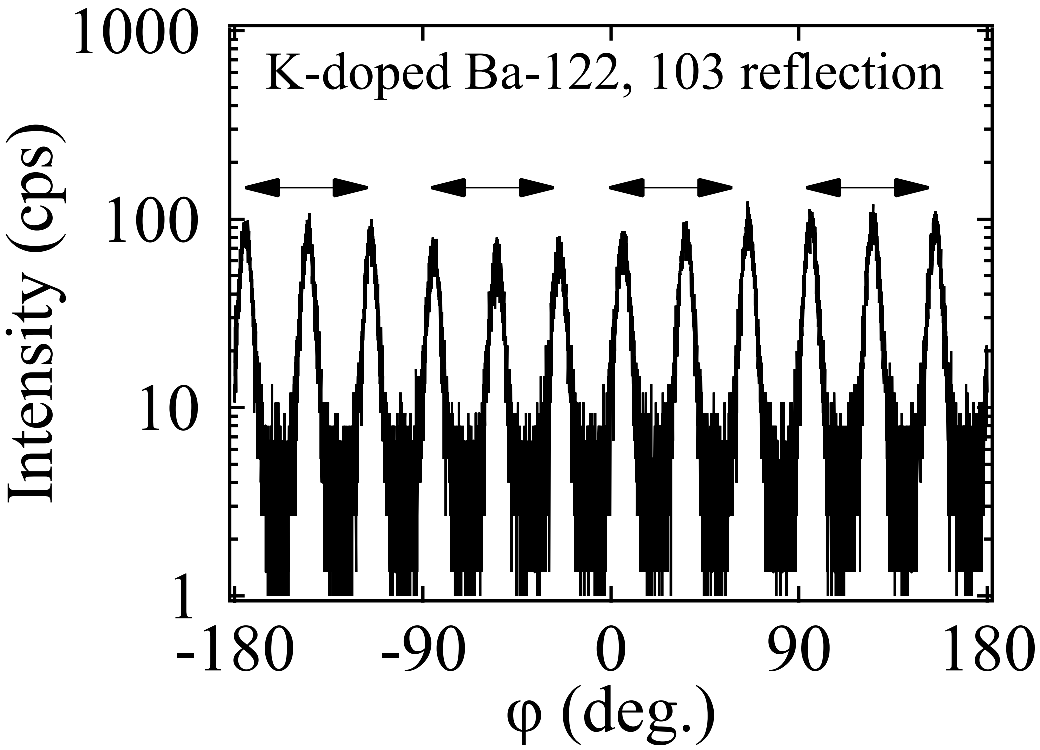

- $(Ba,K)Fe_2As_2$ was not epitaxially grown -> due to the low growth temperature (cf. 800°C for Co-[1] and P-doped[2] Ba122)
- 30° rotated grains were present

[1] T. Katase *et al.*, *SuST* **25**, 084015 (2012).
[2] S. Adachi *et al.*, *SuST* **25**, 105015 (2012).

Strategy for K-doped Ba122 on MgO

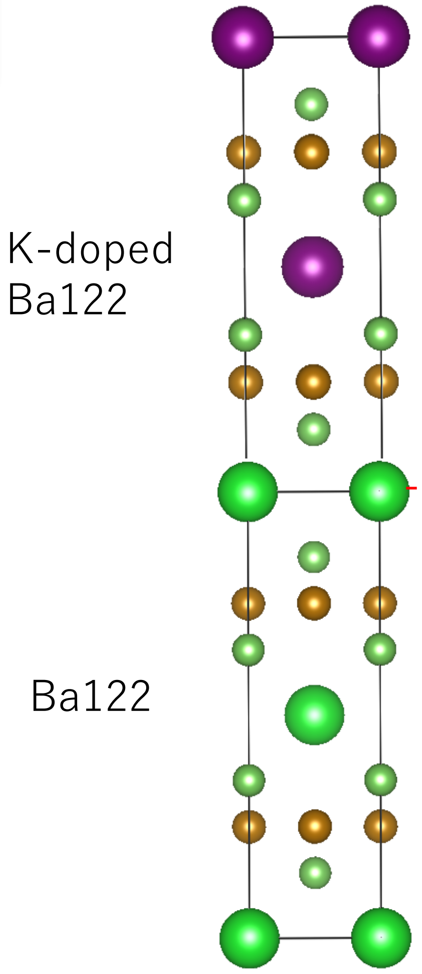

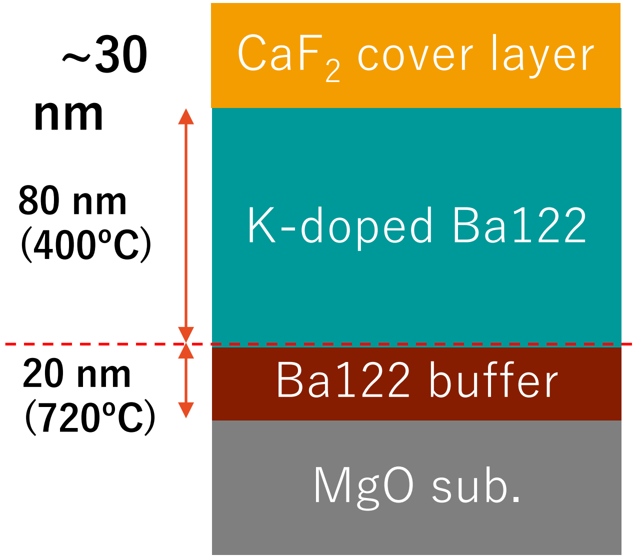

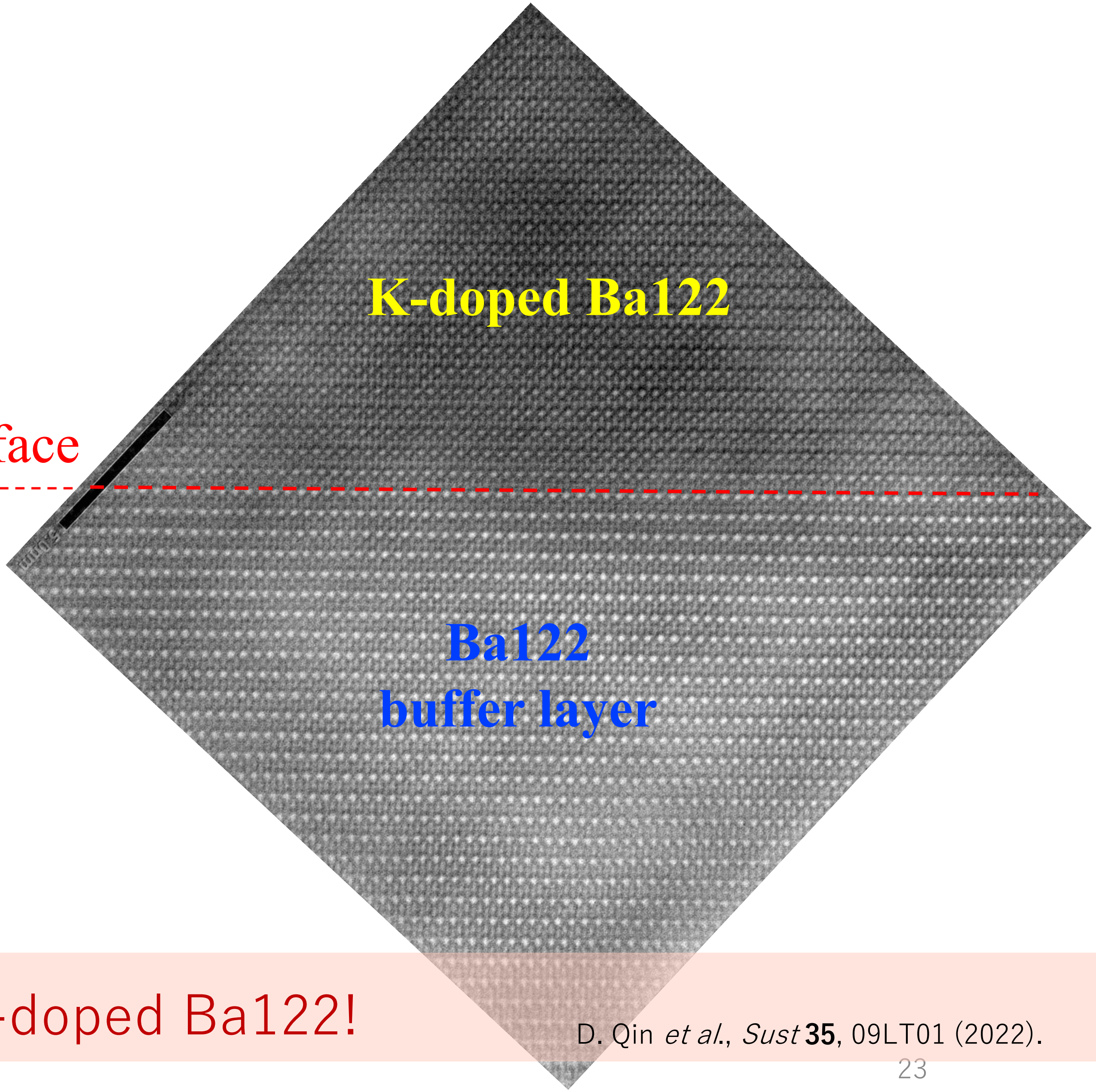

Sharp interface between Ba122 and K-doped Ba122!

D. Qin *et al.*, *Sust* **35**, 09LT01 (2022).

K-doped Ba122 grown on Ba122-buffered MgO(001)

2θ/ω-scan

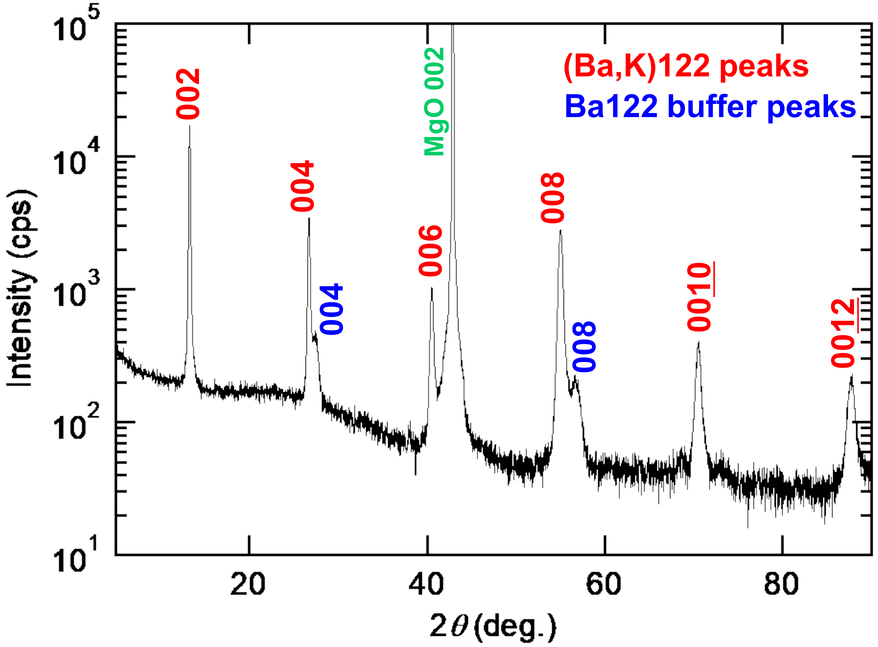

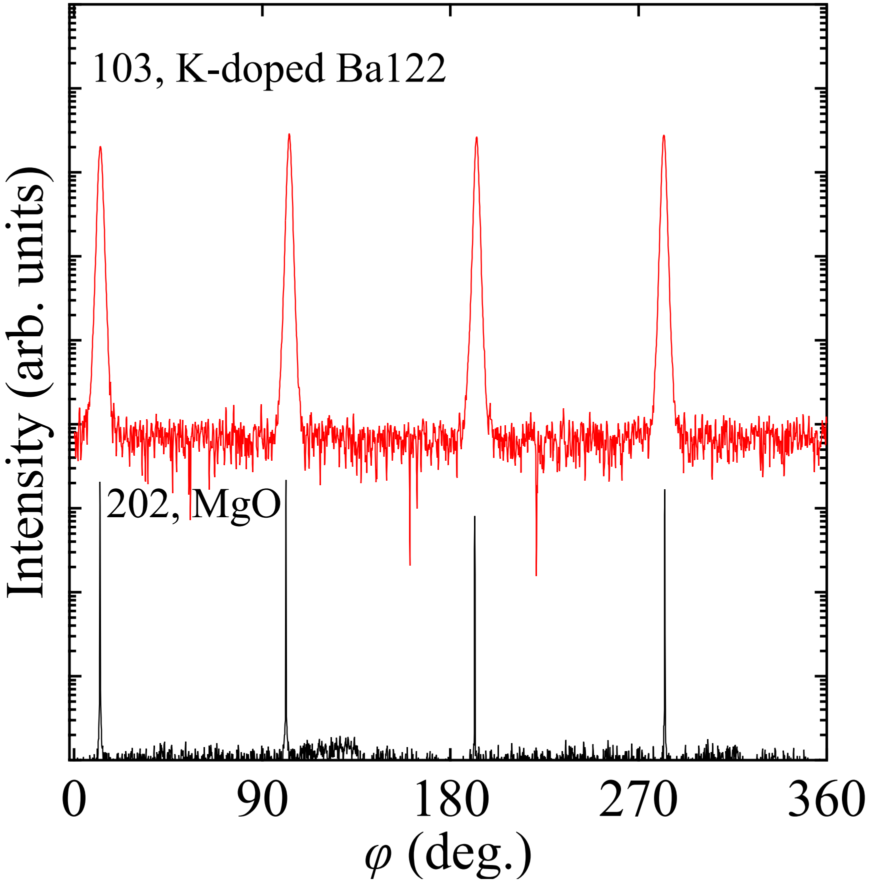

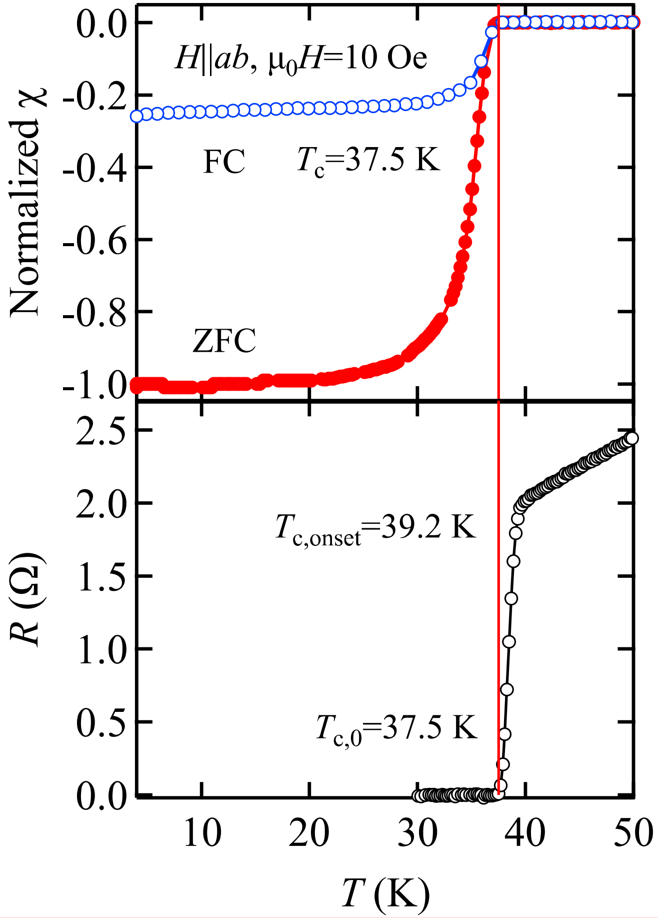

- ➢ The 00*l* peaks arising from K-doped Ba122 and Ba122 were observed
- ➢ K-doped Ba122 was grown epitaxially on Ba122-buffered MgO
- ➢ T_c of K-doped Ba122 was 37.5 K

K-doped Ba122 bicrystals are realised

$\theta_{\mathrm{GB}}=\underline{13^{\circ}}$

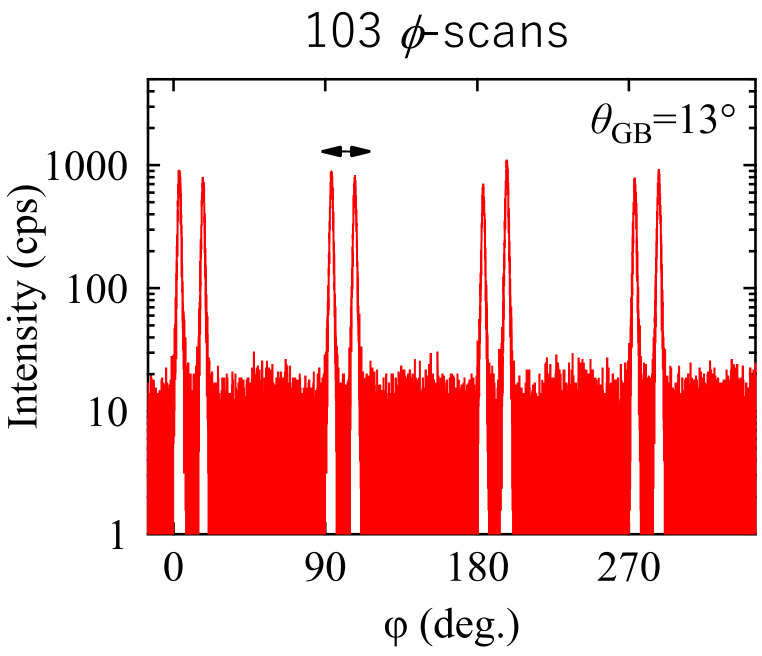

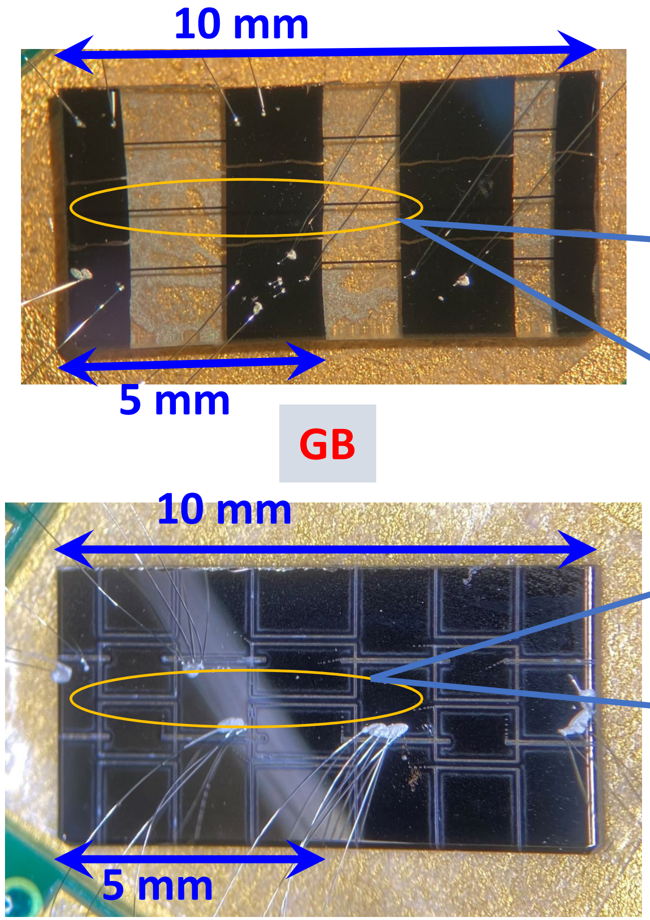

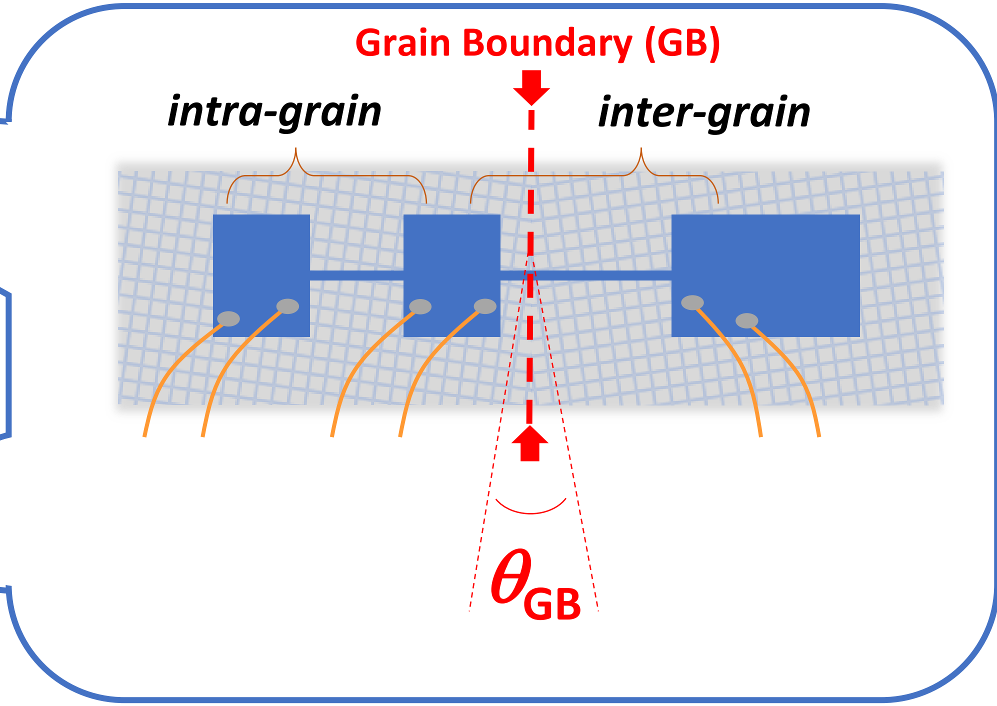

- ➢ Structurally fine K-doped Ba122 films are grown on MgO bi-crystal substrates
- ➢ Microbridge was fabricated by all dry processes (Ar ion etching or laser cutting)

Transport properties of K-doped Ba122 bicrystals

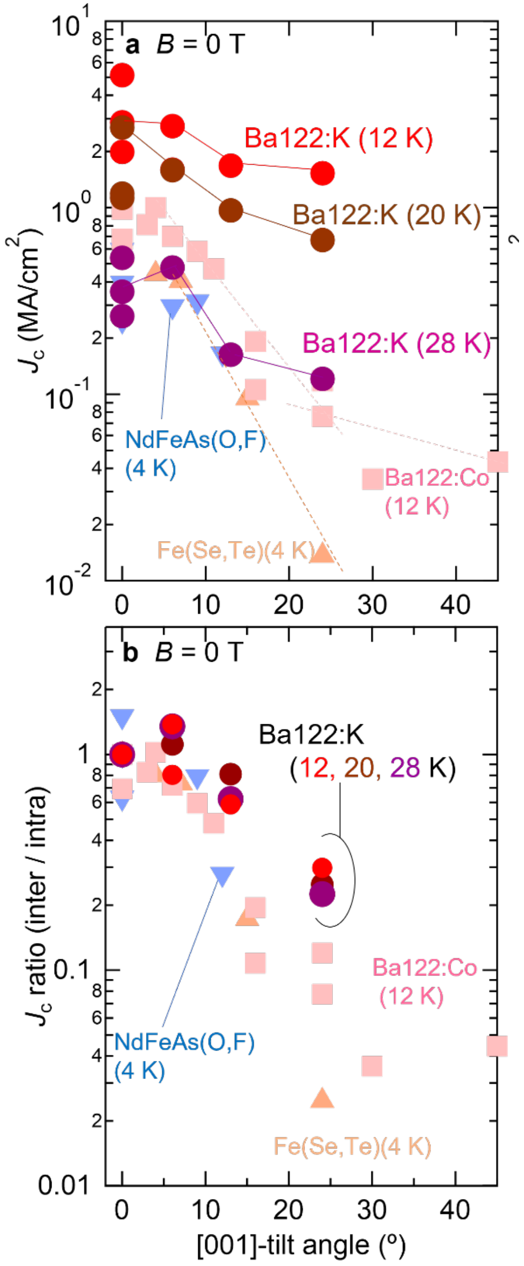

T. Hatano *et al.*, in preparation

- ➢ Even at 12 K and 20 K, inter-grain J_c of K-doped Ba122 is higher than those of other IBS [Co-doped Ba122 (12 K), Fe(Se,Te) (4 K), NdFeAs(O,F) (4 K)]
- ➢ Critical grain boundary angle θ_c of (Ba,K)122 is ~9°, similarly to other

Transport properties of K-doped Ba122 bicrystals

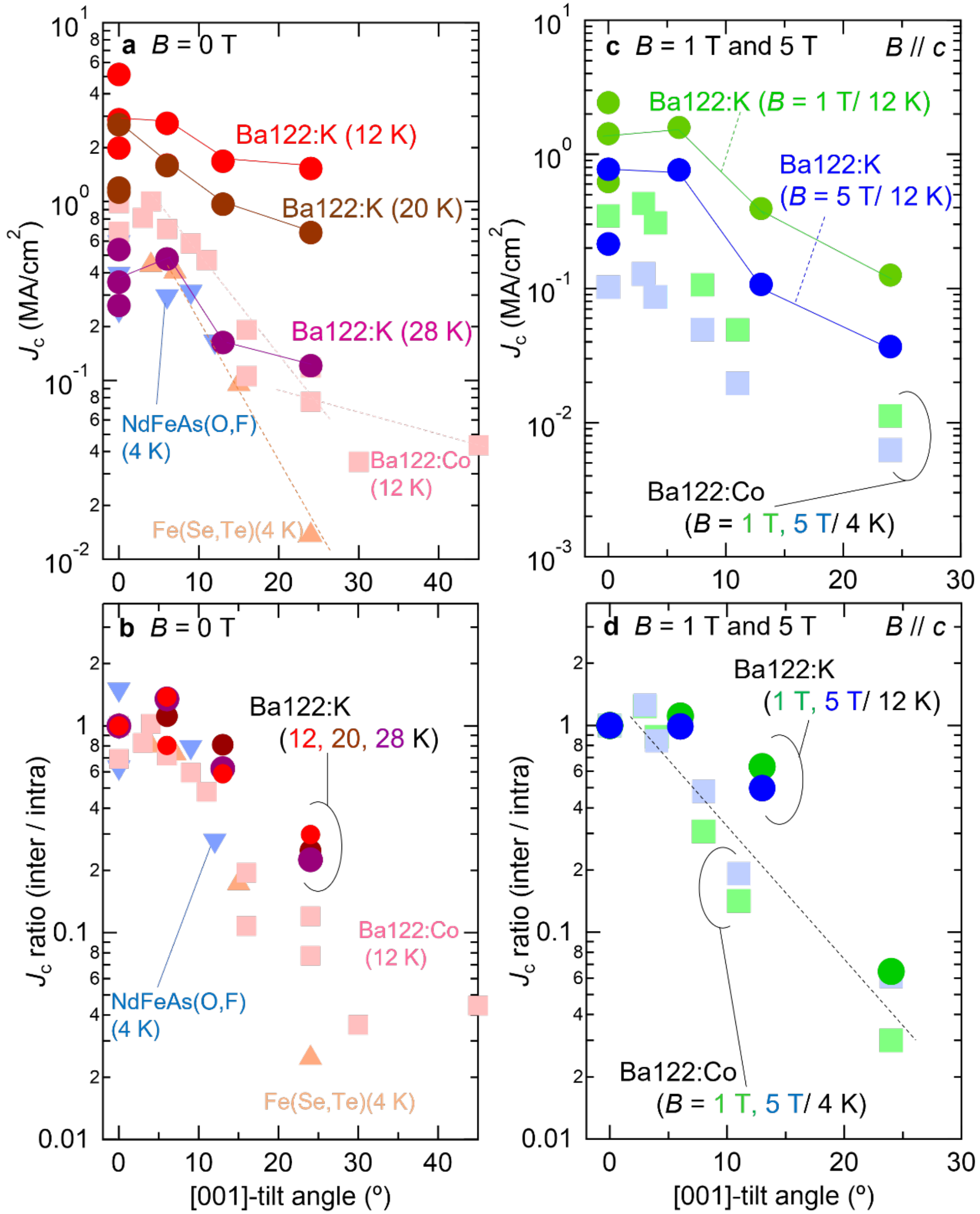

T. Hatano *et al.*, in preparation

- ➢ Even at 12 K and 20 K, inter-grain J_c of K-doped Ba122 is higher than those of other IBS [Co-doped Ba122 (12 K), Fe(Se,Te) (4 K), NdFeAs(O,F) (4 K)]
- ➢ Critical grain boundary angle θ_c of (Ba,K)122 is ~9°, similarly to other IBS
- ➢ The θ_c of (Ba,K)122 is unchanged by applied magnetic fields (c.f. Co-doped Ba122)

Summary

1. Over-doped NdFeAsO showed a high J_c and low anisotropy
   -> The strategy for over-doping method can be applicable
2. Low angle GBs and their networks work as strong pinning centers in K-doped Ba122
3. Inter-grain J_c exceed 1 MA/cm^2 even at θ_{GB}=24° and 12 K
4. The critical angle θ_c for all IBSs seem to be ~9°
5. The θ_c for K-doped Ba122 is unchanged by magnetic field